microorganisms

MDPI

Article

Synergistic Killing of *Staphylococcus aureus* by Mefloquine and 18β-Glycyrrhetinic Acid

Wenwen Cui [1,2,†], Xintong Jiang [1,†], Junyu Chen [1], Xinyu Chen [1], Lei Wan [3], Xuanyi Ren [1], Ruyi Huang [1], Xinxin Feng [3,*] and Huan Yang [1,*]

[1] Xuzhou Key Laboratory of Laboratory Diagnostics, School of Medical Technology, Xuzhou Medical University, Xuzhou 221004, China
[2] Microbiology Laboratory, Xuzhou Center for Disease Control and Prevention, Xuzhou 221000, China
[3] Institute of Chemical Biology and Nanomedicine, State Key Laboratory of Chemo/Biosensing and Chemometrics, Hunan Provincial Key Laboratory of Biomacromolecular Chemical Biology, School of Chemistry and Chemical Engineering, Hunan University, Changsha 410012, China
* Correspondence: xinxin_feng@hnu.edu.cn (X.F.); yangh@xzhmu.edu.cn (H.Y.)
† These authors have contributed equally to this work.

Abstract

Infections caused by *Staphylococcus aureus*, specifically methicillin-resistant *S. aureus* (MRSA), pose a significant clinical challenge due to their inherent drug resistance. Drug repurposing which involves leveraging clinically approved agents with well-established safety profiles—offers a time- and cost-efficient strategy to bridge this therapeutic gap. This study investigates the synergistic antibacterial effects of the combination of 18β-glycyrrhetinic acid (18β-GA) and mefloquine hydrochloride (Mef) against MRSA, and elucidates the underlying molecular mechanisms of this combination. Our results revealed that the Mef+18β-GA combination effectively promotes anti-MRSA activity by disrupting biofilm integrity and suppressing the expression of key virulence genes, thereby significantly impairing both bacterial proliferation and pathogenicity. Transcriptomic analysis showed that the combination treatment globally modulated gene expression via downregulation of key virulence regulators (*agr*), adhesion-related genes (*clfA*, *clfB*, *atl* and *fib*), and antioxidant genes (*katE*, *norB* and *msrB*). We further validated the expression levels of *clfA*, *sigB*, *katE* and *agrA* by RT-qPCR. In a mouse skin infection model, the Mef+18β-GA combination mitigated skin lesions, reduced inflammatory cytokine levels (IL-1β and IL-6), and efficiently removed MRSA from local lesions and systemic organs. Collectively, these findings indicate that 18β-GA and mefloquine act synergistically against MRSA by targeting bacterial growth, biofilm maturation, antioxidant stress responses, and virulence gene expression. This study provides a promising, translationally relevant drug-repurposing combinatorial strategy for the clinical management of MRSA infections, offering the advantages of proven safety and rapid clinical translatability.

Keywords: *Staphylococcus aureus*; MRSA; synergistic antibacterial activity; 18β-glycyrrhetinic acid; mefloquine hydrochloride; virulence

Check for updates

Academic Editor: Hideo Kato

Received: 29 June 2026
Revised: 6 November 2026
Accepted: 11 November 2026
Published: 18 November 2026

Copyright: © 2026 by the authors. Licensee MDPI, Basel, Switzerland. This article is an open access article distributed under the terms and conditions of the Creative Commons Attribution (CC BY) license.

1. Introduction

Staphylococcus aureus is a widespread pathogen responsible for hospital-acquired infections and can cause a range of diseases, including cellulitis, endocarditis, and sepsis [1,2]. Although antibiotics initially provided an effective means of controlling bacterial infections, their rampant misuse has led to the emergence of drug-resistant strains, severely

complicating clinical management. Among these, methicillin-resistant *S. aureus* (MRSA) is of particular concern, with high prevalence in intensive care units [3]. In addition to resistance to methicillin and other β-lactam antibiotics, MRSA is increasingly linked to reduced susceptibility to vancomycin, a drug further constrained by its nephrotoxicity risk [4,5]. Developing safer and more effective therapeutic strategies is therefore urgently needed. Combination therapy, with considerable success achieved in oncology, represents a promising strategy in antimicrobial treatment. Synergistic effects can be achieved by combining different antibiotics or pairing antimicrobials with non-antibacterial agents, and thereby synergistic effects can be achieved, enhancing efficacy while potentially delaying the development of resistance.

Glycyrrhiza, a well-documented herbal plant, exhibits prominent anti-inflammatory, antioxidant, and antiviral properties, which makes it extensively applicable in clinical settings [6,7]. 18β-Glycyrrhetinic acid (18β-GA), which is a pentacyclic triterpenoid compound isolated from *Glycyrrhiza*, is the principal bioactive component responsible for the herb's diverse pharmacological effects and has thus garnered extensive research interest. Accumulating evidence suggests that 18β-GA exerts potent antitumor, antiviral, and antibacterial effects [8–10]. Specifically, it has been shown that this compound inhibits the migration and invasion of gastric cancer cells [11]. In a murine model of mouse hepatitis virus (MHV) infection, 18β-GA inhibited the virus-triggered HMGB1/TLR4 immunoregulatory cascade, thereby effectively mitigating liver inflammatory damage induced by viral hepatitis [12]. In vitro assays have further verified that 18β-GA can robustly inhibit the viability of *Neisseria gonorrhoeae* and abrogate its biofilm formation [13]. Further, 18β-GA induces a dose-dependent inhibition of MRSA growth, accompanied by reduced expression of key virulence genes including *saeR*, *mecA*, and *sbi*. Long et al. showed that high-dose 18β-GA kills community-associated MRSA, while sub-lethal 18β-GA represses virulence genes and without reducing bacterial burdens [14]. Metabolomic analyses indicate sub-lethal 18β-GA remodels MRSA metabolism. Though incapable of eradicating biofilm-resident MRSA, it impairs bacterial micro-aggregation [15]. Notably, monotherapy with this compound tends to induce bacterial resistance; however, combination therapy can mitigate such resistance development, underscoring a promising therapeutic strategy for clinical practice.

Mefloquine hydrochloride (Mef), a synthetic 4-quinolinemethanol derivative, is widely used in treating malaria [16]. A decade-long surveillance report issued by the World Health Organization (WHO) indicated the frequent application of this agent in combination with artesunate for the treatment of plasmodium falciparum infections [17]. Recent investigations have shown that the pharmacological activities of Mef are not limited to its antimalarial effects, but include potential anticancer applications [18]. Further, emerging research suggests that it can serve as an antibiotic adjuvant and enhance the antibacterial efficacy of conventional antibiotics via synergistic interactions [19,20]. Specifically, Mef disrupts the cell membrane structure of *Acinetobacter baumannii* and significantly enhances bactericidal activity when combined with polymyxin B [21].

To the best of our knowledge, no studies have yet investigated the therapeutic efficacy of a combined regimen of 18β-glycyrrhetinic acid (18β-GA) and Mef against MRSA. Our study demonstrate that the Mef+18β-GA combination exerts synergistic bactericidal activity against MRSA by disrupting bacterial membrane integrity, suppressing biofilm formation, inducing excessive ROS accumulation, and downregulating global virulence gene expression. In a murine skin infection model, the combination effectively alleviated skin lesions, reduced inflammatory cytokine levels, and eradicated both local and systemic bacterial burden. Our findings provide an innovative and safe combinatorial strategy for the control of MRSA infections.

2. Materials and Methods

2.1. Materials and Bacterial Strains

S. aureus ATCC 29213 was purchased from the American Type Culture Collection and MRSA was isolated and preserved in our laboratory. Results of the MRSA drug susceptibility assays are presented in Supplementary Tables S1 and S2. Tryptic Soy Broth (TSB, Qingdao Hope Bio-Technology Co., Ltd., Qingdao, China), Tryptic Soy Agar (TSA, Qingdao Hope Bio-Technology Co., Ltd., Qingdao, China) medium, MH Broth (Qingdao Hope Bio-Technology Co., Ltd., Qingdao, China), BHI Broth (Qingdao Hope Bio-Technology Co., Ltd., Qingdao, China) and Brain Heart Infusion Agar (Qingdao Hope Bio-Technology Co., Ltd., Qingdao, China) were used to cultivate all *S. aureus* strains. 18β-Glycyrrhetinic acid and Mefloquine hydrochloride were purchased from MedChemExpress LLC (Shanghai, China).

2.2. Determination of the Minimum INHIBITORY Concentration (MIC)

Minimum inhibitory concentration (MIC) values were determined via broth microdilution following the guidelines of the Clinical and Laboratory Standards Institute (CLSI). Briefly, *Staphylococcus aureus* was cultured overnight, then sub-cultured into fresh MH medium. When the OD_{600} reached 0.6, the bacterial suspension was adjusted to a working inoculum of 5×10^5 CFU/mL. For the sterile 96-well microplate, 100 μL of bacterial suspension was added to wells of rows 1–8. Subsequently, 100 μL of 18β-GA or mefloquine working solution was added to row 1 and mixed thoroughly by pipetting. A total of 100 μL of the mixture from row 1 was transferred to row 2 for serial two-fold dilution. This serial dilution procedure was repeated down to row 8, and 100 μL of the mixture from each well of row 8 was discarded. Each compound was tested in technical duplicates. The final drug concentrations across rows 1 to 8 were 128, 64, 32, 16, 8, 4, 2, and 0 μg/mL, respectively. The microplate was incubated at 37 °C for 16 h, and the MIC was defined as the lowest drug concentration that visibly inhibited bacterial growth.

2.3. Checkerboard Assay for Fractional Inhibitory Concentration Index (FICI)

The checkerboard assay was employed to evaluate the synergistic antibacterial efficacy of 18β-GA and Mef. Briefly, bacteria were cultured to the logarithmic growth phase and subsequently adjusted to a final density of 5×10^5 CFU/mL using MH broth. Two-fold serial dilutions of 18β-GA and Mef were prepared in a 96-well microtiter plate microplate, followed by the addition of 100 μL of the standardized bacterial suspension to each well, and incubated for 16–18 h at 37 °C. The combination MIC was designated as the minimal concentration that completely inhibited visible bacterial growth post-incubation. The fractional inhibitory concentration (FIC) index was calculated using the corresponding formula to characterize the interaction mode between the two agents. The interaction was categorized based on the FIC value: synergism (FIC $\leq$ 0.5), additive effect (0.5 < FIC $\leq$ 1), indifference (1 < FIC $\leq$ 2), and antagonism (FIC > 2).

$$\mathrm{FIC} = \frac{\mathrm{A(MIC\ of\ combination)}}{\mathrm{A(MIC\ of\ alone)}} + \frac{\mathrm{B(MIC\ of\ combination)}}{\mathrm{B(MIC\ of\ alone)}} \quad (1)$$

2.4. Time–Kill Assay

The time–kill assay was used to verify the synergistic effect of 18β-GA and Mef. ATCC 29213 and MRSA were diluted in BHI at the concentration of 5×10^5 CFU/mL and then treated with 16 ug/mL 18β-GA, 8 ug/mL Mef, and 16 ug/mL 18β-GA+8 ug/mL Mef. DMSO was incubated as control. After 0, 2, 4, 6, 8, 10, 12, 14, 16, 18, 20, and 24 h of incubation, the OD_{600} values of bacterial suspensions were measured to plot curves. Simultaneously, 100 µL of bacterial suspension was serially diluted, spread onto BHI plates, and incubated at 37 °C for 16–20 h for colony counting to quantify viable bacteria.

2.5. Detection of Bacterial Biofilm Formation Capacity

The effect of the drug on MRSA biofilm formation was detected using the crystal violet staining method. The logarithmic-phase bacterial suspension was diluted to 5×10^5 CFU/mL and then treated with 16 ug/mL 18β-GA, 8 ug/mL Mef, and 16 ug/mL 18β-GA+8 ug/mL Mef. DMSO was incubated as control. After the 96-well plate was incubated at 37 °C for 20 h, the supernatant was discarded and gently washed three times with PBS. Each well was then filled with 200 µL of 0.1% crystal violet solution and incubated at room temperature in the dark for 15 min. The staining solution was discarded, and the wells were washed three times with PBS. Afterward, 200 µL of 95% ethanol was added to each well, and the plate was shaken at room temperature for 10 min for decolorization. The absorbance at 590 nm was measured using a microplate reader (Bio-Rad, Hercules, CA, USA).

2.6. Reactive Oxygen Species (ROS) Generation

The level of ROS was detected using a Cell Reactive Oxygen Species Detection Kit (Jiangsu KeyGEN BioTECH Corp., Ltd, Nanjing, China). MRSA in the logarithmic phase was diluted to 5×10^5 CFU/mL and treated with 18β-GA and Mef at 37 °C for 2 h. Subsequently, the bacterial suspensions were centrifuged at 5000 rpm for 5 min, and then washed three times with PBS. A fluorescent probe was added into bacterial suspensions and incubated in the dark at 37 °C for 30 min. After incubation, the sample was centrifuged at 5000 rpm for 5 min; the supernatant was discarded and washed three times with PBS. Finally, 350 µL of PBS was added to resuspend the bacteria, and a fluorescence microplate reader (BioTek Instruments, Inc., Winooski, VT, USA) was used to measure the fluorescence intensity (excitation wavelength of 485 nm; emission wavelength of 528 nm).

2.7. Thiourea Scavenger Rescue Experiment

For thiourea-mediated ROS rescue assays, bacterial inoculum was adjusted to 5×10^5 CFU/mL and divided into four treatment arms: negative control (NC), mefloquine alone, 18β-GA alone, and Mef+18β-GA combination. Each group received thiourea at a final concentration of 1 mmol/L and was mixed completely. Parallel groups in the absence of thiourea were assessed in preliminary trials; the addition of 1 mmol/L thiourea itself exerted no discernible effect on MRSA growth. All samples were incubated at 37 °C for 24 h. After incubation, bacterial suspensions were serially diluted and plated onto agar for CFU enumeration.

2.8. Bacterial Morphological Observation (Scanning Electron Microscopy, SEM)

Staphylococcus aureus in the logarithmic growth phase was diluted to 5×10^5 CFU/mL and underwent different treatments at 37 °C for 2 h. A 100 µL aliquot of bacterial suspension from each experimental group was taken, serially diluted, and spread onto solid BHI agar plates, which were then incubated overnight at 37 °C. Sterile cover slips were placed over the bacterial colonies on the agar plates, and the bacteria were incubated overnight to allow bacterial adhesion to the cover slip surfaces. The cover slips were removed and placed in 2.5% glutaraldehyde fixative for 30 min at room temperature. They were then washed three times with 0.1 M PBS for 15 min each. Subsequently, the samples were fixed with 1% osmium tetroxide in the dark at room temperature for 1–2 h, followed by three 15 min rinses with PBS. Dehydration was performed using a graded ethanol series (30%, 50%, 70%, 80%, 90%, 95%, 100%, and 100%) and isoamyl acetate for 15 min each. The dehydrated samples underwent critical point drying, were sputter-coated with gold, and were then observed and photographed using a scanning electron microscope (Hitachi-SU8100, Hitachinaka, Ibaraki, Japan).

2.9. Reverse-Transcription Quantitative PCR (RT-qPCR)

Total bacterial RNA was extracted using an RNA extraction kit(VICMED, Huanggang, China) following the manufacturer's instructions (VICMED, VR605). The concentration of RNA was determined by a NanoDrop spectrophotometer (Merinton Instruments (Beijing) Co., Ltd., Beijing, China). First-strand cDNA was synthesized from 300 ng of total RNA using a reverse transcription kit(Takara Bio Inc., Kusatsu, Shiga, Japan). Quantitative real-time PCR was performed on a real-time PCR system (Roche, LightCycler® 96 System, Roche Diagnostics GmbH, Mannheim, Germany) with SYBR Green qPCR Master Mix (Selleck.cn, B21202, Selleck Chemicals LLC, Houston, TX, USA). Thermal cycling was performed with an initial preheating step at 95 °C for 5 min. The amplification stage consisted of 45 cycles: 95 °C for 20 s, 60 °C for 20 s, 72 °C for 20 s, and 78 °C for 1 s. Melting curve analysis was carried out as follows: 95 °C for 10 s, 65 °C for 60 s, and 97 °C for 1 s, followed by a cooling step at 37 °C for 30 s. Relative gene expression levels of *agrA*, *clfA*, *katE* and *sigB* were calculated by the $2^{-\Delta\Delta Ct}$ method, with the housekeeping gene 16S serving as the internal reference. All experiments were performed in three independent biological replicates. Primer sequences for target and reference genes are listed in Supplementary Table S3.

2.10. Bacterial Adhesion and Invasion Assays

2.10.1. Cell Adhesion Assay

293T and Hela cells were cultured in Dulbecco's modified Eagle's High-glucose medium (DMEM-H, Gbico) supplemented with 10% fetal bovine serum (FBS, Gbico), 100 U/mL penicillin and 0.1 mg/mL streptomycin (Gbico). Cells were maintained in a humidified incubator (37 °C, 5% CO2, HeracellTM 150i, Thermo Scientific, Langenselbold, Germany). Before bacterial adhesion, MRSA was diluted to 5×10^5 CFU/mL, and incubated with different concentrations of 18β-GA and Mef at 37 °C for 2 h. 293T and HeLa cells (2×10^5 cells/well) received 200 µL of bacterial suspension (MOI = 50), while the control groups were treated with DMSO. After being cocultured in a 5% CO_2, 37 °C incubator for 2 h, the plates were gently washed three times with precooled PBS. Each well was treated with 0.25% trypsin-EDTA to detach adherent cells. The cell suspension was serially diluted and spread onto TSB agar plates, followed by incubation at 37 °C for 18 h. Colony counts within the 30–300 CFU range were recorded to calculate the bacterial adhesion per cell (CFU/mL).

2.10.2. Cell Invasion Assay

The bacterial pretreatment and cell culture were the same as those in Section 2.10.1. In the experimental group, 200 μL of bacterial suspension (MOI = 50) was added and incubated under 5% CO_2 at 37 °C for 3 h. The supernatant was discarded, and the cells were washed three times with precooled PBS. Each well was then supplemented with DMEM containing 200 μg/mL gentamicin and cultured for 2 h. After three PBS washes, 1 mL of 0.1% Triton X-100 lysis buffer was added to each well and left at room temperature for 5 min, followed by vortexing for 1 min to lyse the cells and release the intracellular invasive bacteria. The cell lysate was serially diluted, and 100 μL of the diluted solution was spread onto TSB agar plates. After incubation at 37 °C for 18 h, the number of colonies within the 30–300 CFU range was counted to quantify bacterial invasive ability.

2.11. Transcriptome Sequencing and Bioinformatics Analysis

Staphylococcus aureus from different drug treatment groups and the control group were collected, washed with PBS, and pelleted via centrifugation at 4000 rpm and then sent to Shanghai Majorbio Biopharm Technology Co., Ltd. (Majorbio) for prokaryotic transcriptome sequencing. The raw sequencing data were subjected to quality control and filtering, followed by sequence assembly. The assembled unigene sequences were submitted to public databases for functional annotation, including the Gene Ontology (GO) database and the Kyoto Encyclopedia of Genes and Genomes (KEGG) database. Bacterial resistance genes and virulence genes were annotated using the Comprehensive Antibiotic Resistance Database (CARD) and the Virulence Factors of Pathogenic Bacteria Database (VFDB), respectively. Differential gene expression analysis was performed using DESeq2 software(Version 1.42.0), with $|\log_2 FC| \geq 1$ and padjust < 0.05 as the criteria to screen for differentially expressed genes (DEGs).

A total of 12 transcriptome samples were sequenced in this study, generating 40.61 Gb of clean data. Each sample produced more than 2.95 Gb of clean data, supporting sufficient sequencing depth for downstream transcriptomic analysis. All samples exhibited reliable base quality, with Q30 values above 96.07%, ensuring high-quality sequencing data. The mapping rate of clean reads to the *S. aureus* reference genome ranged from 90.34% to 95.71%.

2.12. Skin Infection Model

The fur on the dorsal skin of mice was removed using depilatory cream. After disinfection of the injection site, mice were subcutaneously (s.c.) inoculated with 100 μL of *Staphylococcus aureus* suspension at a concentration of 5×10^8 CFU/mL. At 6 h post-infection (hpi), 100 μL of the drug solution was administered subcutaneously at a site 0.5 mm adjacent to the infected lesion including NC (saline), Mef (5 mg/kg), 18β-GA (10 mg/kg), Mef (5 mg/kg) + 18β-GA combination (10 mg/kg) and vancomycin (16 mg/kg). Subsequently, the same combination regimen was administered subcutaneously once daily for 7 days. On day 7 post-infection, the length and width of the lesions were measured. The lesion area was calculated by multiplying the length by the width (expressed in mm^2). Mice were then euthanized. To determine the bacterial burden, skin lesions, spleen, and lungs were harvested and weighed. Each 0.1 g tissue sample was homogenized using a high-throughput tissue homogenizer in 0.3% Triton solution. The homogenates were serially diluted with PBS and plated onto LB agar plates, and colony-forming units (CFU) were counted. All animal experiments were conducted following the institutional and national guidelines and approved by the Institutional Animal Care and Use Committee of Xuzhou Medical University (202602T013).

2.13. Enzyme-Linked Immunosorbent Assay (ELISA)

Skin lesions were collected and weighted. Each 0.1 g tissue sample was lysed in RIPA lysis buffer (WB3100, NCM Biotech) supplemented with a protease inhibitor cocktail (VP1012, VicMed). The lysate was centrifuged at 12,000 rpm for 15 min, and the supernatant was collected. The concentrations of IL-1β and IL-6 in the supernatants were measured using a non-coating mouse ELISA kit purchased from Invitrogen (Carlsbad, CA, USA).

2.14. Hematoxylin and Eosin (H&E) Staining

Prepared paraffin sections were deparaffinized and rehydrated. Hematoxylin staining was performed, followed by differentiation and bluing to clearly visualize cell nuclei. The sections were then dehydrated in graded ethanol and stained with eosin to demonstrate cytoplasmic structures. Subsequently, the sections were dehydrated in graded ethanol, cleared in xylene, and mounted with neutral balsam. All sections were observed and imaged under an upright optical microscope (Nikon Eclipse E100, Nikon Corporation, Tokyo, Japan) equipped with an image acquisition system (Nikon DS-U3, Japan).

2.15. Statistical Analysis

All experimental data were statistically analyzed using GraphPad Prism 9.0 software, with at least three independent biological replicates used for each sample. The experimental results are expressed as the mean ± standard deviation (mean ± SD). Comparisons among multiple groups were performed using one-way ANOVA combined with multiple comparison tests while the comparison between two groups was conducted using the unpaired *t*-test. The criteria for determining statistical significance were as follows: $p < 0.05$ indicated statistically significant differences, whereas $p \geq 0.05$ indicated no statistically significant differences.

3. Results

3.1. Synergistic Antibacterial Activity Screening of Mef+18β-GA Combination Against MRSA

The checkerboard method was used to determine the combined antibacterial effects of different concentrations of 18β-GA and Mef. The results revealed that when used alone, the MIC of 18β-GA against both ATCC29213 and MRSA was 64 μg/mL, whereas the MIC of Mef against both strains was 32 μg/mL (Table 1). After combination therapy, the MICs of both drugs significantly declined. The combination of 16 μg/mL GA and 8 μg/mL Mef indicated a distinct synergistic effect between GA and Mef, with an FICI of 0.5. This regimen was consequently used in subsequent experimental investigations (Figure 1A–C). The antibacterial effect was further confirmed by a colony-forming unit (CFU) assay, revealing a significant reduction in MRSA survival following combination treatment (Figure 1D).

Table 1. MIC of 18β-GA and Mef against 3 strains of *Staphylococcus aureus* ($n = 3$).

Sample	18β-GA (ug/mL)	$FIC_{18β\text{-}GA}$	Mef (ug/mL)	FIC_{Mef}
ATCC 29213	64	16	32	8
MRSA 1	64	16	32	8
MRSA 2	64	16	32	8

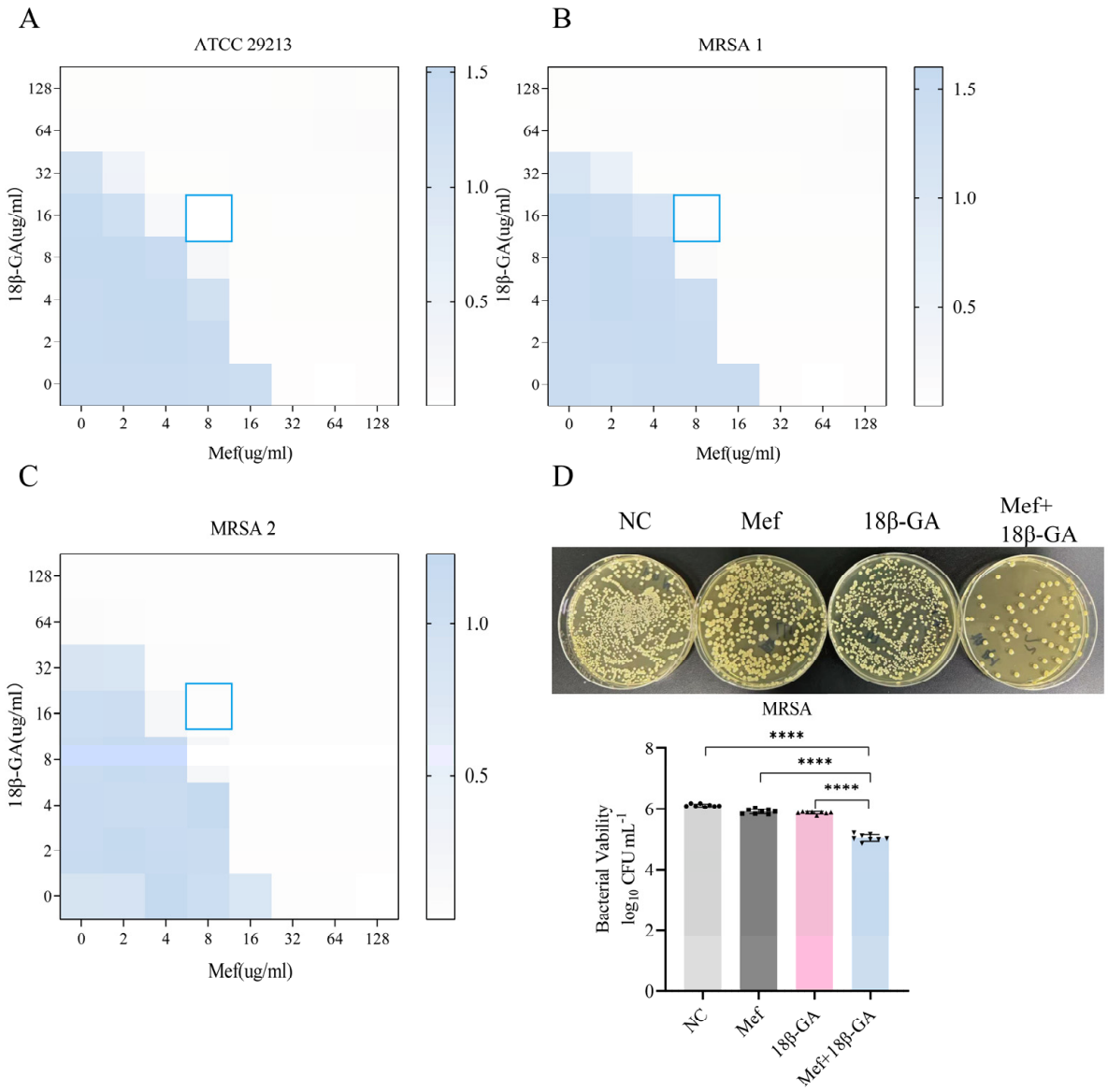


Figure 1. Synergistic antibacterial activity screening of Mef+18β-GA combination against MRSA. Chessboard experiments were performed to detect the combination anti-bacterial effect of 18β-GA and Mef against ATCC29213 (**A**), MRSA 1 (**B**) and MRSA 2 (**C**). The antibacterial effect of 16 ug/mL 18β-GA and 8 ug/mL Mef on MRSA after 2 h treatment (**D**). Data are presented as the means ± SEM ($n = 8$ per group). Statistical significance was determined with one-way ANOVA followed by Tukey's multiple comparisons test, and $p-$values were calculated as follows: **** $p < 0.0001$.

3.2. Mef+18β-GA Combination Suppresses S. aureus Growth and Impairs MRSA Biofilm Formation

To clarify the antibacterial effects of 18β-GA and Mef on *S. aureus*, we examined the growth characteristics of *S. aureus* ATCC 29213 and two MRSA clinical isolates (MRSA 1, MRSA 2) under different treatments by measuring OD_{600} and viable bacterial counts over a 24 h incubation period. As shown in Figure 2A–C, the growth curves indicated that Mef alone and 18β-GA treatment had no obvious inhibitory effect on the growth of the three strains, while the combination of 18β-GA+ Mef produced a robust synergistic growth inhibition, which was further validated by the time–kill assays (Figure 2D–F). The proliferation of ATCC29213 and MRSA was suppressed within 2 h of drug exposure, and this inhibitory effect was sustained for up to 24 h. Relative to Mef, 18β-GA alone only marginally restrained bacterial growth, with no statistically significant effect.

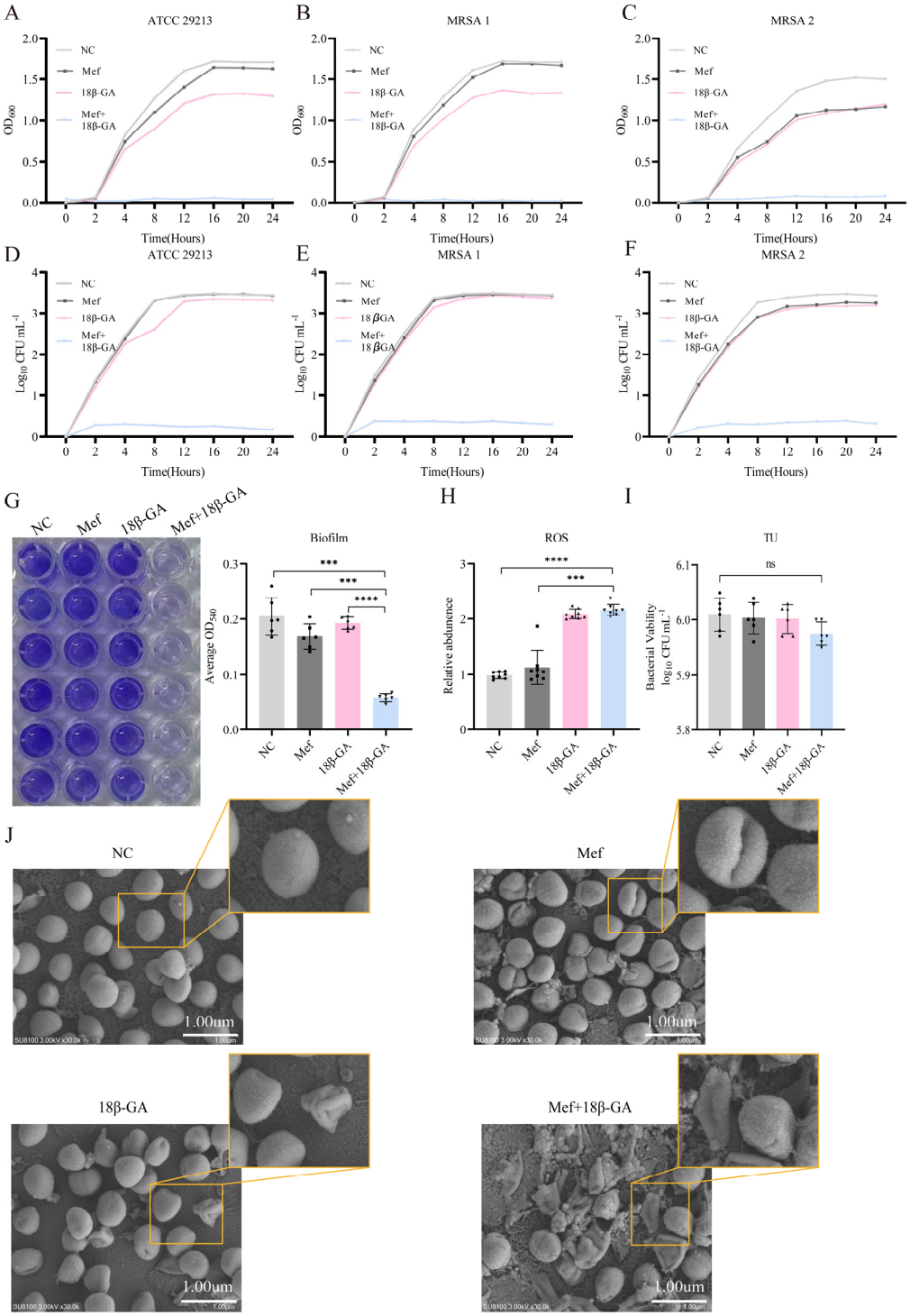


Figure 2. Mef+18β-GA combination suppresses *S. aureus* growth and impairs MRSA biofilm formation. The effects of 16 ug/mL 18β-GA and 8 ug/mL Mef on the growth curve of ATCC29213 (**A**) MRSA 1 (**B**) and MRSA 2 (**C**). The effects of 16 ug/mL 18β-GA and 8 ug/mL Mef on the viable count of ATCC29213 (**D**) MRSA 1 (**E**) and MRSA 2 (**F**); (**G**) 16 ug/mL 18β-GA and 8 ug/mL Mef inhibit biofilm formation ($n = 6$ per group) and (**H**) stimulate ROS generation of MRSA ($n = 8$ per group). Effects of ROS scavenger TU on the antibacterial activity of the combination ($n = 6$ per group) (**I**). SEM images of MRSA treated with 16 ug/mL 18β-GA and 8 ug/mL Mef (**J**). The scale bar represents 1.0 μm. Data are presented as the means ± SEM. Statistical significance was determined with one-way ANOVA followed by Tukey's multiple comparison test, and *p*-values were calculated as follows: *** $p < 0.001$, **** $p < 0.0001$.

As a key determinant of bacterial pathogenicity, biofilms not only facilitate persistent infection and host colonization but also confer robust intrinsic resistance to antibiotics. Herein, we evaluated the modulatory effects of 18β-GA and Mef on MRSA biofilms using crystal violet staining. As displayed in Figure 2G, neither 18β-GA nor Mef alone as monotherapies exerted a significant disruptive effect on MRSA biofilms, whereas their combined administration significantly suppressed biofilm formation. In addition, reactive oxygen species (ROS) staining assays (Figure 2H) showed a considerable increase in intracellular ROS levels in MRSA after combination treatment, indicating the induction of pronounced oxidative stress. Excessive ROS accumulation can cause irreversible oxidative damage to bacterial macromolecules, ultimately triggering cell death. To determine whether the antibacterial activity of Mef combined with 18β-GA depended on ROS production, thiourea (TU), a well-characterized ROS scavenger, was included in the assay. Notably, the antibacterial effect of the Mef + 18β-GA combination regimen was abolished upon TU treatment (Figure 2I), supporting that ROS generation is required for its antibacterial action.

Scanning electron microscopy (SEM) was applied to visualize morphological changes of bacterial cells and biofilm architecture (Figure 2J). NC and Mef-treated groups exhibited intact, spherical *S. aureus* cells with smooth surfaces and dense biofilm matrix. 18β-GA monotherapy induced mild surface deformation of bacterial cells. Importantly, the Mef+18β-GA combination group displayed severe bacterial morphological damage, with collapsed, irregular cells and markedly disrupted biofilm structure.

3.3. Mef+18β-GA Combination Treatment Attenuates MRSA Adhesion and Invasion In Vitro

Adhesion and invasion are key pathogenic mechanisms employed by *S. aureus* during host infection. To investigate the effect of combination treatment on MRSA pathogenicity, this study employed an in vitro cellular model to evaluate the influence of 18β-GA and Mef on MRSA virulence. Colony counting of bacteria recovered from the surface of infected cell membranes revealed that the adhesive capacity of MRSA onto HeLa and 293T cells was significantly reduced after combination treatment (Figure 3A,B). Notably, bacterial invasion into host cells and subsequent intracellular proliferation contribute to the persistence and recurrence of infections. Our findings showed that the combination therapy not only effectively inhibited MRSA adhesion and also attenuated its invasive ability (Figure 3C,D).

3.4. Mef and 18β-GA Combination Therapy Regulates MRSA Antioxidant Stress and Virulence Genes

To further elucidate the molecular mechanisms underlying the antibacterial effect of the combination therapy against MRSA, bacteria were treated with 18β-GA and Mef and we subsequently subjected the bacteria to RNA-seq analysis. A total of 2213 genes were detected in the control group, compared with 2352 genes in the combination treatment group, of which 64 genes were uniquely expressed in the latter (Figure 4A). Compared with the control, the Mef+18β-GA combination group exhibited 738 significantly differentially expressed genes (DEGs) (Figure 4B).

GO and KEGG enrichment analyses were conducted to explore the functional roles of these DEGs. GO enrichment results (Figure 4C) showed that the DEGs were significantly enriched in three primary categories, namely biological process (BP), molecular function (MF), and cellular component (CC). Notably, the most highly enriched terms were associated with plasma membrane, oxidoreductase complex, and membrane. Overall, these findings indicate pronounced alterations in membrane structure and transport capacity in MRSA after combined treatment.

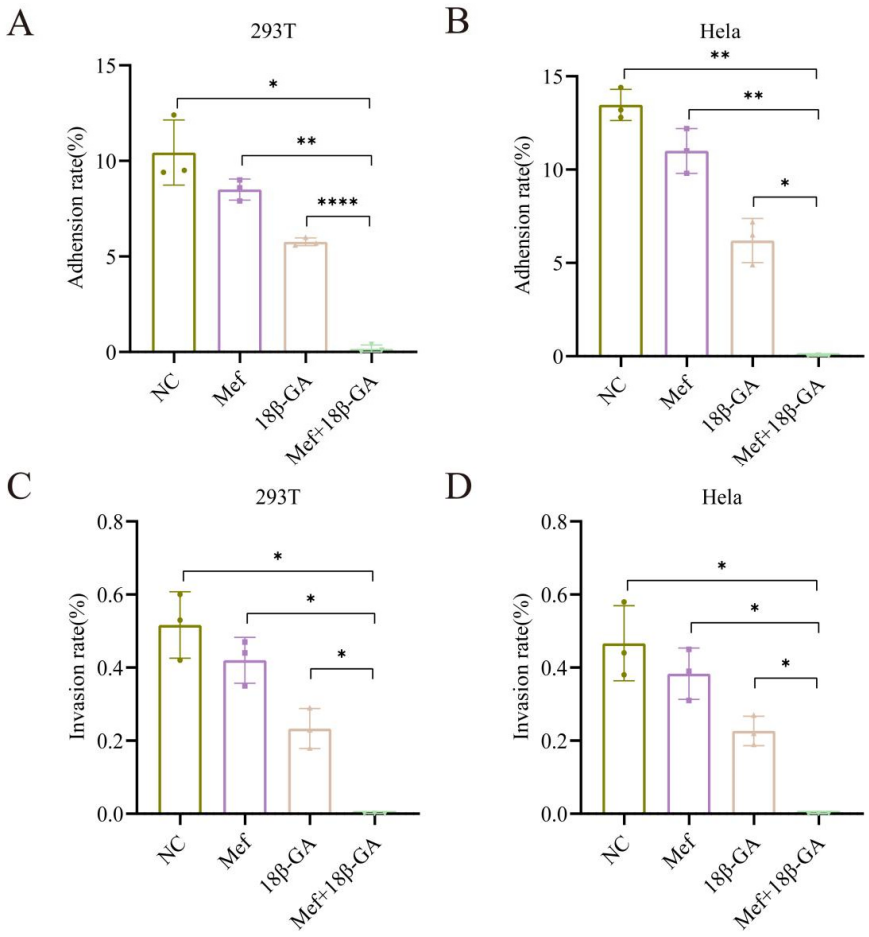


Figure 3. Mef+18β-GA combination therapy attenuates MRSA adhesion and invasion in vitro. The effect of 18β-GA and Mef combined treatment on MRSA adhesion to 293T (**A**) and HeLa cells (**C**) ($n = 3$ per group). The effect of 18β-GA and Mef combined treatment on MRSA invasion of 293T (**B**) and HeLa cells (**D**) ($n = 3$ per group). Data are presented as the means ± SEM. Statistical significance was determined with one-way ANOVA followed by Tukey's multiple comparisons test, and *p*-values were calculated as follows: * $p < 0.05$, ** $p < 0.01$, **** $p < 0.0001$.

For KEGG pathway enrichment analysis, the top 15 significantly enriched pathways were identified for visual presentation (Figure 4D). DEGs were primarily enriched in multiple core pathways, including the two-component system, nitrogen metabolism, arginine biosynthesis, riboflavin metabolism, and fatty acid degradation, which constitute critical signaling cascades and metabolic networks that mediate bacterial adaptive responses and pathogenicity.

Compared with the control group, the combination therapy group exhibited 394 upregulated and 469 downregulated DEGs. The combined treatment significantly downregulated the expression of antioxidant stress-related genes, including *norB*, *katE*, *msrB*, *sigB*, and *osmC*. In addition, there was a significant reduction in the expression of genes encoding virulence factors associated with bacterial adhesion and invasion, such as *clfA/clfB*, *atl*, *fib*, *sdrC_D_E*, *agrA/agrC*, and *psmB* (Figure 4E,F).

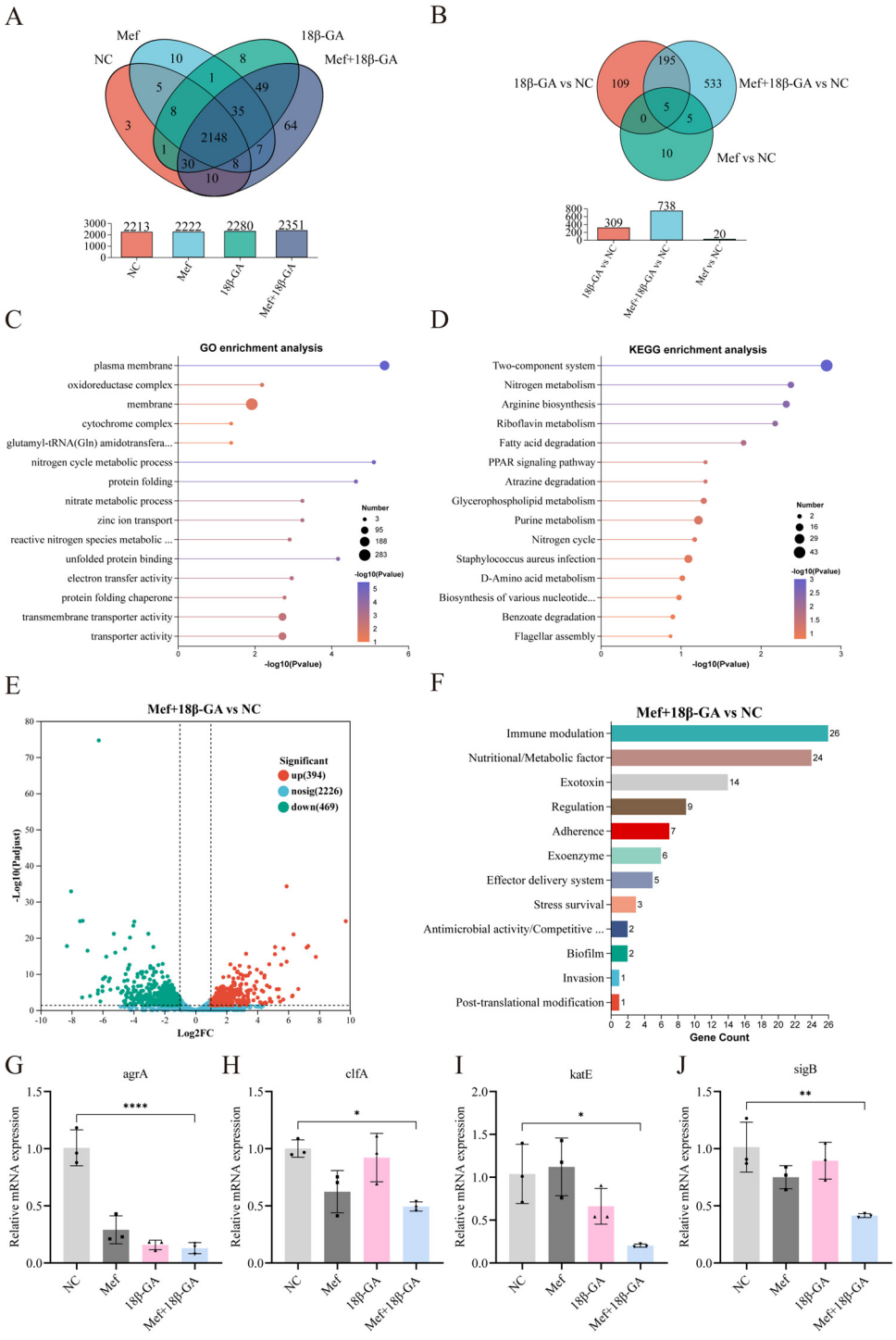


Figure 4. Transcriptomic analysis reveals Mef+18β-GA combination therapy modulates MRSA antioxidant stress and virulence genes. (**A**) Venn map of different groups. (**B**) Geneset Venn map. (**C**) Analysis of GO enrichment pathway (**D**) Analysis of KEGG functional pathway. (**E**) Differential gene volcano map. Vertical dashed lines correspond to $\log_2$ FC = ±1, and the horizontal dashed line indicates adjusted P-value = 0.05. (**F**) Analysis of Virulent Factor Category Level I. (**G-J**) RT-qPCR detection of relative mRNA expression of *agrA*, *clfA*, *katE*, and *sigB*. Data are presented as the means ± SEM ($n = 3$ per group). Statistical significance was determined with one-way ANOVA followed by Tukey's multiple comparisons test, and *p*-values were calculated as follows: * $p < 0.05$, ** $p < 0.01$, **** $p < 0.0001$.

RT-qPCR was conducted to verify the expression of selected virulence and regulatory genes (*agrA*, *clfA*, *katE*, *sigB*). Compared with the NC group, the transcription levels of *agrA*, *clfA*, *katE* and *sigB* were markedly reduced in the Mef, 18β-GA and Mef+18β-GA combination groups, and the suppressive effect was strongest in the combined treatment group (Figure 4G–J). Concurrently, the combination regimen suppresses genes crucial for adhesion and invasion, thereby significantly attenuating MRSA virulence and providing a molecular basis for its observed antibacterial efficacy.

3.5. Mef and 18β-GA Combination Ameliorates Skin Inflammation and Prevents Systemic Bacterial Spread

In this study, we established an *S. aureus*-induced mouse skin infection model to assess the synergistic antibacterial efficacy of Mef in combination with 18β-GA (Figure 5A). Following infection, mice receiving the Mef+18β-GA combination treatment showed significantly alleviated back skin lesions, with marked reductions in erythema, swelling, and ulceration, compared with the negative control (NC) group. Quantitative analysis confirmed that combination therapy drastically reduced lesion areas compared with the NC group (Figure 5B,C). Consistent with these observations, measurement of pro-inflammatory cytokines revealed that Mef+18β-GA combination treatment significantly suppressed IL-6 and IL-1β expression in infected lesion tissues (Figure 5D,E).

To investigate the in vivo therapeutic effect of Mef combined with 18β-GA against *S. aureus* infection, a murine skin abscess model was established, and the experimental workflow is outlined in Figure 5A. At day 7 post-infection, mice in the NC group developed prominent skin abscesses with severe erythema and ulceration. Monotherapy with Mef or 18β-GA moderately attenuated skin lesion severity, while the Mef+18β-GA combination group exhibited markedly shrunken wounds and greatly alleviated inflammatory manifestations, which was comparable to the vancomycin (Van) positive control group (Figure 5B). Quantitative measurement confirmed that the lesion area in the Mef+18β-GA combination group was significantly smaller than that in the NC, Mef-alone and 18β-GA-alone groups (Figure 5C).

In line with the macroscopic observations, the protein levels of pro-inflammatory cytokines IL-6 and IL-1β in lesion homogenates were significantly reduced in the Mef+18β-GA combination group compared with the control and monotherapy groups, indicating that the combined treatment effectively suppressed local inflammatory response (Figure 5D,E).

Importantly, bacterial burden analysis further demonstrated that Mef+18β-GA combination treatment dramatically reduced the bacterial loads in the primary lesion, as well as in the spleen and lung tissues. The combination regimen achieved superior bacterial clearance efficacy relative to single-agent treatment, and effectively inhibited the systemic dissemination of *S. aureus* from the skin infection site to distal organs (Figure 5F–H).

Further, hematoxylin and eosin (HE) staining further confirmed the therapeutic benefits of combination treatment. In contrast to the NC group, which showed severe inflammatory cell infiltration, tissue necrosis, and disrupted epidermal architecture, the Mef+18β-GA combination treatment group exhibited markedly attenuated inflammatory infiltration and preserved normal skin structure (Figure 5I). Collectively, these findings indicate that co-administration of Mef and 18β-GA effectively controls local cutaneous infection, limits systemic bacterial dissemination, and thereby exerts strong synergistic anti-infective and systemic protective effects against *S. aureus* infection.

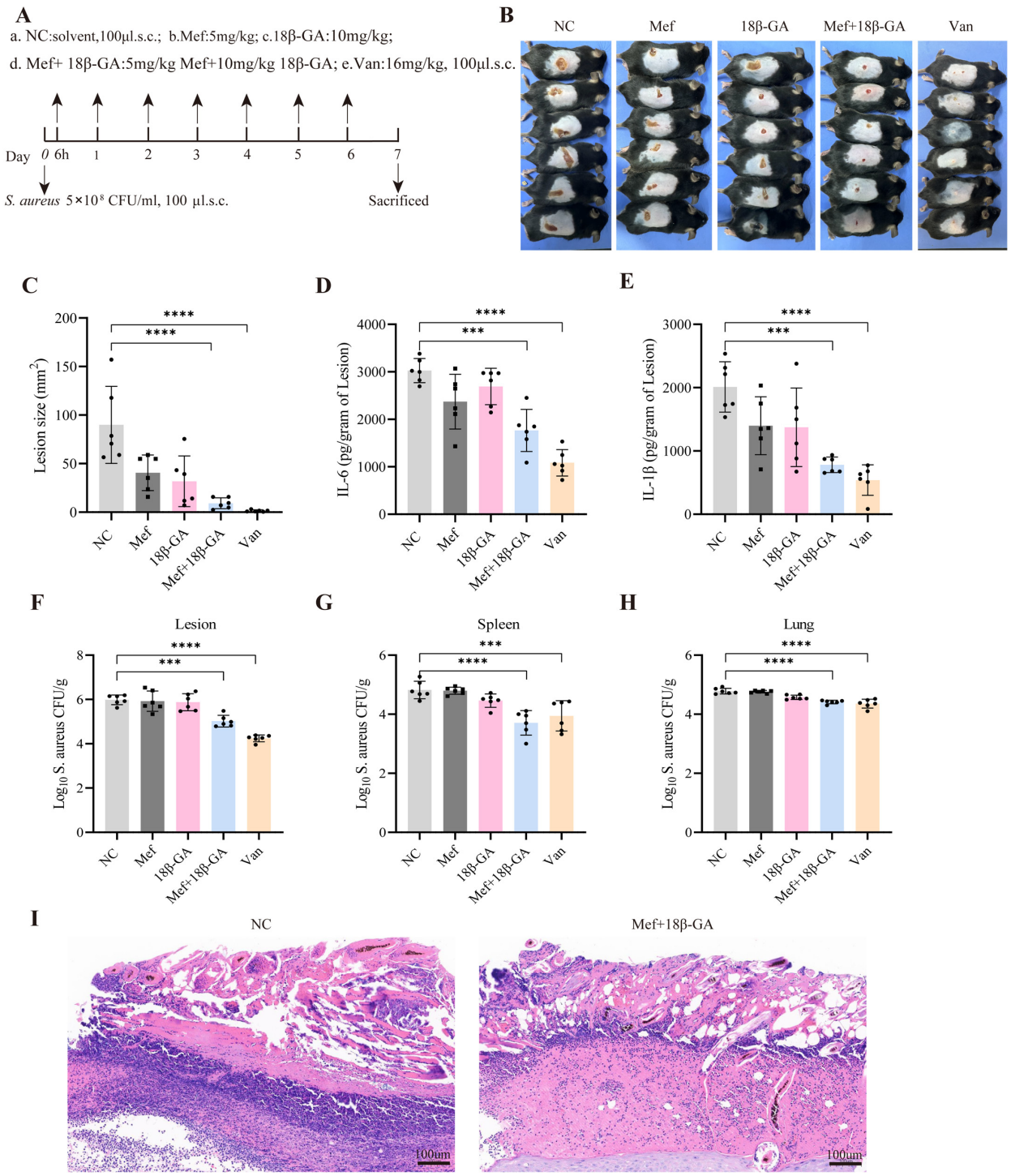


Figure 5. Mef+18β-GA combination ameliorates skin inflammation and prevents systemic bacterial spread in vivo. (**A**) Schematic overview of the experimental timeline and procedures. (**B**,**C**) Representative images of skin lesions at 7 days post-infection and measurement of lesion size ($n = 6$ mice per group). The expression levels of pro-inflammatory cytokines IL-6 (**D**) and IL-1β (**E**) in infected lesion tissues of mice were detected by ELISA ($n = 6$ mice per group). Bacterial loads of *Staphylococcus aureus* in lesion (**F**), spleen (**G**) and lung (**H**) tissues of mice ($n = 6$ mice per group). (**I**) Representative HE staining images of skin tissues from mice in each group (scale bar: 100 μm). Data represent mean ± SEM. Statistical significance was determined with one-way ANOVA followed by Tukey's multiple comparisons test, and p-values were calculated as follows: *** $p < 0.001$, **** $p < 0.0001$. Complete source data are available as Source Data.

4. Discussion

The global spread of MRSA poses a severe threat to public health, making the development of novel therapeutic strategies an urgent need [22]. Vancomycin, a critical drug in the clinical treatment of *S. aureus* infections, is often regarded as the "last line of defense". Nevertheless, the rising incidence of vancomycin-resistant strains in recent years has further intensified pressures on clinical therapy [23,24]. Combination therapy with natural products and repurposed drugs represents a promising approach to enhancing efficacy and reducing resistance development. This study revealed that Mef+18β-GA combination suppresses MRSA proliferation and disrupts biofilm architecture, and it also effectively attenuates bacterial virulence, thereby reducing its capacity to adhere to and invade host cells.

The resistance of MRSA to β-lactam antibiotics is essentially mediated by the acquisition of the mecA gene, which encodes the penicillin-binding protein *PBP2a*, along with resistance endowed through the production of β-lactamases that hydrolyze the drugs [25,26]. Clinically, the prolonged use of a single antibiotic promotes the selection of resistance mutations, whereas combination therapies—by targeting different signaling pathways—often produce synergistic effects and enhance antimicrobial activity [27,28]. Studies have confirmed that extracts derived from traditional Chinese medicines exert inhibitory activity against MRSA [29]. The natural compound 18β-GA has previously been shown to inhibit the growth of *S. aureus* in a dose-dependent manner [14]. In this study, 18β-GA alone exhibited limited antibacterial activity. Mef, although commonly used for malaria treatment, has been proposed as an antibiotic adjuvant to potentiate antimicrobial efficacy. The findings of this study are consistent with the conclusions of the aforementioned works, confirming that the combined use of 18β-GA and Mef can exert significant synergistic antibacterial effects, while significantly reducing the effective drug concentrations of both. Notably, the Mef+18β-GA combination is effective against the standard strain ATCC 29213, and it also exhibits potent antibacterial activity against clinical MRSA isolates. When used alone, glycyrrhetinic acid gradually suppressed the growth of ATCC 29213 and MRSA over time; however, when combined with Mef, the onset of antibacterial action was significantly accelerated, with combined treatment inhibiting bacterial proliferation in vitro within 2 h.

Biofilm formation is a central process associated with both the pathogenicity and drug resistance of MRSA. The extracellular matrix barrier constructed by biofilms effectively shields bacterial cells from environmental stress and antibiotic attack [30]. Further, recent research has proposed a "trick-bacteria-with-bacteria" strategy to break this barrier—chemically modifying and inactivating bacteria to serve as targeted drug carriers that penetrate biofilms and release antibiotics on demand [31]. Previous studies have confirmed that glycyrrhetinic acid can significantly inhibit biofilm formation in *Pseudomonas aeruginosa* [32] and *Streptococcus mutans* [33]. Additionally, this natural product clearly has a concentration-dependent inhibitory activity against *S. aureus* biofilms [15]. On this basis, the present study aimed to investigate whether Mef could synergistically enhance the disruption of MRSA biofilms when combined with 18β-GA. The results showed that the combination of Mef and 18β-GA almost completely inhibited the formation of MRSA biofilms. SEM further confirmed that the combined treatment not only reduced adhesion and aggregation among MRSA cells and it also directly disrupted the spatial architecture of the biofilms, causing dissolution of the bacterial cell wall and leakage of intracellular contents. The structural integrity of biofilms is critical to bacterial survival advantages and pathogenic capacity. The biofilm-disrupting effects of the combined treatment may interfere with bacterial quorum sensing communication and cooperation, thereby significantly diminishing the overall survival and pathogenic capabilities of MRSA [34].

Biofilm formation is regulated by global regulatory systems, including the quorum sensing systems including *Agr* and *LuxS*, the transcription factor *SigB*, and the accessory reg-

ulator *SarA*. The *Agr* quorum-sensing system comprises *agrABCD* and its effector molecule *RNAIII* [35]. Previous research has shown that agr-deficient *S. aureus* exhibits significantly enhanced biofilm-forming capacity [36]. In this study, transcriptomic analysis revealed that combined drug treatment significantly downregulated the expression of *agrA* and *agrC* in MRSA, while *agrB* expression showed an upward trend, implying that the drug combination of 18β-GA and Mef interferes with signal transduction in the *Agr* quorum-sensing circuit. Further, *SigB* and *SarA* can regulate biofilm formation by inhibiting nuclease and protease activities [37]. Among these regulators, the *σB* factor encoded by *sigB* serves as a global transcriptional regulator in Gram-positive bacteria, and its activity is tightly controlled by the upstream *rsbU/V/W* operon [38]. Under normal growth conditions, *σB* remains inactive by binding to *rsbW*. Upon exposure to external stress, *rsbW*-mediated inhibition is relieved, facilitating association with RNA polymerase and initiating transcription of genes involved in biofilm formation and virulence expression [39]. This study revealed that the combined treatment downregulated the expression of both *sigB* and *rsbW*, indicating disruption of the transcription-coupled regulatory mechanism within the σ^B-*rsbU/V/W* complex. These results collectively confirm that the drug combination exerts multi-target and multilayered regulatory effects on MRSA.

Biofilm formation is a dynamic, multistage process involving bacterial attachment, aggregation, maturation, and dispersal, involving various virulence factors that play critical roles throughout the process [40,41]. Of these, surface adhesin proteins, such as fibronectin-binding proteins (*FnBPs*), clumping factors (*Clfs*), elastin-binding proteins (*Ebps*), and autolysin (*Atl*), serve as key mediators of bacterial attachment to substrates [42]. In this study, combination therapy upregulated the expression of the adhesin-encoding genes *fnbA* and *fnbB* in MRSA, while significantly downregulating *fib*, *clfA/clfB*, *arlR*, and *atl*. These findings indicate that the treatment exerts multifaceted regulatory effects on bacterial adhesion. Cell-based assays further confirmed that the combination therapy markedly reduced the adhesion and invasion efficiency of MRSA toward 293T and HeLa cells, thereby offering direct evidence that this combination regimen attenuates MRSA pathogenicity.

Furthermore, the *icaR* gene serves as a negative regulator of the *ica* operon, and its downregulation generally relieves repression of the extracellular polysaccharide synthesis pathway, thereby promoting biofilm formation and maturation [43]. Here, combination therapy significantly increased *icaR* expression, highlighting another potential mechanism whereby it suppresses MRSA biofilm formation. In summary, by targeting the regulation of several biofilm-related signaling pathways and functional genes, combination therapy can interfere with the biofilm formation process of MRSA in multiple dimensions. However, the complexity of its regulatory mechanisms warrants further in-depth analysis.

ROS accumulation is a key mechanism underlying the bactericidal action of many antimicrobial agents. Excessive intracellular ROS levels can induce oxidative damage, resulting in bacterial cell death. Notably, 18β-GA has been established to exhibit potent anti-inflammatory activity. Cai et al. showed that 18β-GA suppresses the invasion and metastasis of gastric cancer cells via the ROS/protein kinase C-α (PKC-α)/ERK signaling pathway [11]. In our study, combination therapy was found to significantly increase ROS levels in MRSA. Although no prior reports have directly linked 18β-GA to antibacterial effects through modulation of bacterial ROS pathways, our findings suggest that oxidative stress likely contributes to the antimicrobial activity of the combined treatment. Further, bacterial ROS metabolism is closely related to the evolution of antibiotic resistance. Previous studies have shown that bacteria can enhance their antioxidant defense systems to adapt to high-ROS environments, thereby increasing their tolerance to antimicrobial agents [44]. Thiourea tests confirmed ROS generation is a primary bactericidal driver, not a secondary cell-death by-product, implying that oxidative stress contributes substantially to

the combined antimicrobial effect. Transcriptomic data offer a molecular explanation for this oxidative burst: the combination significantly downregulated a suite of antioxidant defense genes, including an oxidative stress peroxidase (*katE*), as well as the stress regulator *sigB*, which controls expression of multiple antioxidant genes [45,46]. Impairment of the bacterial antioxidant defense system would leave cells unable to detoxify endogenously generated ROS, leading to irreversible oxidative damage to proteins, DNA, and lipids, and ultimately cell death.

Our KEGG pathway enrichment analysis revealed that differentially expressed genes (DEGs) were predominantly involved in two-component systems, nitrogen metabolism, arginine biosynthesis, riboflavin metabolism, and fatty acid degradation. Two-component systems are the primary means by which bacteria sense and respond to environmental cues, including antibiotic stress and host signals; their dysregulation would severely impair MRSA adaptive capacity [4]. Nitrogen metabolism and arginine biosynthesis are central to bacterial growth, cell wall synthesis, and redox homeostasis [47]. Fatty-acid degradation pathways, by contrast, are intimately associated with membrane lipid homeostasis and energy generation, which aligns with the membrane-damaging phenotype observed in our experiments. Together, these transcriptomic alterations indicate that the Mef+18β-GA combination disrupts core metabolic networks that support bacterial growth, stress resistance, and pathogenicity.

Mef+18β-GA combination downregulated *agrA*, *clfA*, *katE* and *sigB*, which govern quorum sensing and stress tolerance. Repressed *agrA* reduces bacterial dispersal and invasiveness, while suppressed *sigB* weakens biofilm-associated stress resistance. The combination of Mef and 18β-GA downregulates the transcriptional expression of *katE*, thereby impairing the resistance of *Staphylococcus aureus* to oxidative stress-mediated killing. In line with these transcriptional changes, the combination impaired MRSA adherence and invasion toward host cells via downregulating adhesin-encoding genes such as *clfA*, thereby attenuating infective potential.

Using an *S. aureus*-induced mouse skin infection model, we demonstrated that the Mef +18β-GA combination exerts robust therapeutic efficacy in vivo. Combination treatment significantly reduced lesion size, suppressed local production of pro-inflammatory cytokines, and efficiently cleared bacteria from skin lesions as well as systemic organs. Importantly, inclusion of monotherapy groups (18β-GA alone, Mef alone) confirmed that neither agent alone produced comparable therapeutic benefit, verifying that the in vivo efficacy reflects synergistic interaction.

Several limitations of this study should be acknowledged. First, while we confirmed synergy in two MRSA isolates, the number of clinical strains tested remains limited. Second, the present work focused on efficacy endpoints; detailed pharmacokinetic studies and systematic toxicity evaluations are needed to support clinical translation. Third, although we confirmed the causal role of ROS using scavenger experiments, deeper functional validation using gene knockout or overexpression strains is required. Fourth, adhesion and invasion assays were performed using immortalized cell lines rather than primary human epithelial cells, which may more faithfully recapitulate the natural host–pathogen interface; future work should confirm these findings in more physiologically relevant cellular models.

Collectively, our in vivo results verify that the Mef +18β-GA combination exerts potent synergistic effects against *S. aureus*-induced skin infection by simultaneously enhancing bacterial clearance, suppressing excessive inflammatory responses, and inhibiting systemic bacterial dissemination. Effective anti-staphylococcal therapy is reliant on the dual targeting of both pathogens and host-driven inflammation [48,49]. The combination demonstrates encouraging anti-MRSA activity, warranting follow-up pharmacokinetic, dose-optimization and toxicity studies for future translation.

Supplementary Materials: The following supporting information can be downloaded at: https://www.mdpi.com/article/10.3390/microorganisms14112677/s1. Table S1: MRSA1 Antimicrobial susceptibility test results; Table S2: MRSA2 Antimicrobial susceptibility test results; Table S3: Primers used for RT-qPCR.

Author Contributions: Methodology, W.C., L.W., X.R. and R.H.; Formal analysis, W.C.; Data curation, X.J., J.C. and X.C.; Writing—original draft, W.C., X.J., J.C. and X.C.; Writing—review & editing, X.F. and H.Y.; Funding acquisition, X.F. and H.Y. All authors have read and agreed to the published version of the manuscript.

Funding: This work was supported by the China Postdoctoral Science Foundation (Grant Nos. 2022M712681 and 2025T180402), the Jiangsu Provincial Natural Science Foundation (Grant No. BK20231170), the Jiangsu Training Program of Innovation and Entrepreneurship for Undergraduates (Grant No. S202510313087), the Student Science and Technology Innovation Project of the National Demonstration Center for Experimental Basic Medical Science Education (Xuzhou Medical University) (Grant No. 2024BMS03), the National Natural Science Foundation of China (Grant No. 22177031), and the Science and Technology Program of Hunan Province (Grant No. 2026QK3056).

Institutional Review Board Statement: The study was approved by the Institutional Animal Care and Use Committee of Xuzhou Medical University (protocol code 202602T013 and approval date 8 February 2026).

Informed Consent Statement: Not applicable.

Data Availability Statement: The RNA-seq data have been deposited in the Genome Sequence Archive, CRA037631. All remaining data generated or analyzed in this study are provided in the Source Data file. Source data are provided with this paper.

Conflicts of Interest: The authors declare no competing interests.

References

1. Tong, S.Y.C.; Davis, J.S.; Eichenberger, E.; Holland, T.L.; Fowler, V.G. Staphylococcus aureus Infections: Epidemiology, Pathophysiology, Clinical Manifestations, and Management. *Clin. Microbiol. Rev.* **2015**, *28*, 603–661. [CrossRef] [PubMed]
2. Turner, N.A.; Sharma-Kuinkel, B.K.; Maskarinec, S.A.; Eichenberger, E.M.; Shah, P.P.; Carugati, M.; Holland, T.L.; Fowler, V.G., Jr. Methicillin-resistant Staphylococcus aureus: An overview of basic and clinical research. *Nat. Rev. Microbiol.* **2019**, *17*, 203–218. [CrossRef] [PubMed]
3. Lakhundi, S.; Zhang, K. Methicillin-Resistant Staphylococcus aureus: Molecular Characterization, Evolution, and Epidemiology. *Clin. Microbiol. Rev.* **2018**, *31*, e00020-18. [CrossRef] [PubMed]
4. Cheung, G.Y.C.; Bae, J.S.; Otto, M. Pathogenicity and virulence of *Staphylococcus aureus*. *Virulence* **2021**, *12*, 547–569. [CrossRef] [PubMed]
5. Cong, Y.; Yang, S.; Rao, X. Vancomycin resistant Staphylococcus aureus infections: A review of case updating and clinical features. *J. Adv. Res.* **2020**, *21*, 169–176. [CrossRef] [PubMed]
6. Wang, J.; Chen, X.; Wang, W.; Zhang, Y.; Yang, Z.; Jin, Y.; Ge, H.M.; Li, E.; Yang, G. Glycyrrhizic acid as the antiviral component of Glycyrrhiza uralensis Fisch. against coxsackievirus A16 and enterovirus 71 of hand foot and mouth disease. *J. Ethnopharmacol.* **2013**, *147*, 114–121. [CrossRef] [PubMed]
7. Khan, S.F.; Shetty, B.; Fazal, I.; Khan, A.M.; Mir, F.M.; Moothedath, M.; Vj, R.; Muhamood, M. Licorice as a herbal extract in periodontal therapy. *Drug Target Insights* **2023**, *17*, 70–77. [CrossRef] [PubMed]
8. Gupta, V.K.; Fatima, A.; Faridi, U.; Negi, A.S.; Shanker, K.; Kumar, J.; Rahuja, N.; Luqman, S.; Sisodia, B.S.; Saikia, D.; et al. Antimicrobial potential of Glycyrrhiza glabra roots. *J. Ethnopharmacol.* **2008**, *116*, 377–380. [CrossRef] [PubMed]
9. Li, W.; Asada, Y.; Yoshikawa, T. Antimicrobial flavonoids from Glycyrrhiza glabra hairy root cultures. *Planta Med.* **1998**, *64*, 746–747. [CrossRef] [PubMed]
10. Chin, Y.; Jung, H.; Liu, Y.; Su, B.-N.; Castoro, J.A.; Keller, W.J.; Pereira, M.A.; Kinghorn, A.D. Antioxidant Constituents of the Roots and Stolons of Licorice (*Glycyrrhiza glabra*). *J. Agric. Food Chem.* **2007**, *55*, 4691–4697. [CrossRef] [PubMed]
11. Cai, H.; Chen, X.; Zhang, J.; Wang, J. 18B-glycyrrhetinic acid inhibits migration and invasion of human gastric cancer cells via the ROS/PKC-α/ERK pathway. *J. Nat. Med.* **2018**, *72*, 252–259. [CrossRef] [PubMed]
12. Shi, X.; Yu, L.; Zhang, Y.; Liu, Z.; Zhang, H.; Zhang, Y.; Liu, P.; Du, P. Glycyrrhetinic acid alleviates hepatic inflammation injury in viral hepatitis disease via a HMGB1-TLR4 signaling pathway. *Int. Immunopharmacol.* **2020**, *84*, 106578. [CrossRef] [PubMed]

13. Zhao, Y.; Su, X. Antibacterial activity of 18β-glycyrrhetinic acid against Neisseria gonorrhoeae in vitro. *Biochem. Biophys. Rep.* **2023**, *33*, 101427. [CrossRef] [PubMed]
14. Long, D.R.; Mead, J.; Hendricks, J.M.; Hardy, M.E.; Voyich, J.M. 18B-Glycyrrhetinic acid inhibits Methicillin-Resistant staphylococcus aureus survival and attenuates virulence gene expression. *Antimicrob. Agents Chemother.* **2013**, *57*, 241–247. [CrossRef] [PubMed]
15. Yamashita, T.; Kawada-Matsuo, M.; Katsumata, T.; Watanabe, A.; Oogai, Y.; Nishitani, Y.; Miyawaki, S.; Komatsuzawa, H. Antibacterial activity of disodium succinoyl glycyrrhetinate, a derivative of glycyrrhetinic acid against Streptococcus mutans. *Microbiol. Immunol.* **2019**, *63*, 251–260. [CrossRef] [PubMed]
16. Kucharski, D.J.; Jaszczak, M.K.; Boratyński, P.J. A review of modifications of quinoline antimalarials: Mefloquine and (hydroxy)Chloroquine. *Molecules* **2022**, *27*, 1003. [CrossRef] [PubMed]
17. WHO. *Report on Antimalarial Drug Efficacy, Resistance and Response: 10 Years of Surveillance (2010–2019)*; World Health Organization: Geneva, Switzerland, 2020.
18. Tao, Q.; Liu, N.; Wu, J.; Chen, J.; Chen, X.; Peng, C. Mefloquine enhances the efficacy of anti-PD-1 immunotherapy via IFN-γ-STAT1-IRF1-LPCAT3-induced ferroptosis in tumors. *J. Immunother. Cancer* **2024**, *12*, e8554. [CrossRef] [PubMed]
19. Podoll, J.; Olson, J.; Wang, W.; Wang, X. A Cell-Free screen for bacterial membrane disruptors identifies mefloquine as a novel antibiotic adjuvant. *Antibiotics* **2021**, *10*, 315. [CrossRef] [PubMed]
20. Liang, X.; Liu, Z.; Wang, Y.; Zhang, Y.; Deng, W.; Liu, Q.; Lu, Z.; Li, K.; Chang, Y.; Wei, L. Progress in the study of mefloquine as an antibiotic adjuvant for combination bacterial inhibition treatment. *Front. Cell. Infect. Microbiol.* **2024**, *14*, 1470891. [CrossRef] [PubMed]
21. Tharmalingam, N.; Jayanthan, H.S.; Port, J.; Rossatto, F.C.P.; Mylonakis, E. Mefloquine reduces the bacterial membrane fluidity of *Acinetobacter baumannii* and distorts the bacterial membrane when combined with polymyxin B. *mBio* **2025**, *16*, e0401624. [CrossRef] [PubMed]
22. Mediavilla, J.R.; Chen, L.; Mathema, B.; Kreiswirth, B.N. Global epidemiology of community-associated methicillin resistant Staphylococcus aureus (CA-MRSA). *Curr. Opin. Microbiol.* **2012**, *15*, 588–595. [CrossRef] [PubMed]
23. Micek, S.T. Alternatives to vancomycin for the treatment of Methicillin-Resistant staphylococcus aureus infections. *Clin. Infect. Dis.* **2007**, *45*, S184–S190. [CrossRef] [PubMed]
24. Amberpet, R.; Sistla, S.; Sugumar, M.; Nagasundaram, N.; Manoharan, M.; Parija, S.C. Detection of heterogeneous vancomycin-intermediate Staphylococcus aureus. *Indian. J. Med. Res.* **2019**, *150*, 194–198. [CrossRef] [PubMed]
25. Uehara, Y. Current Status of Staphylococcal Cassette Chromosome mec (SCCmec). *Antibiotics* **2022**, *11*, 86. [CrossRef] [PubMed]
26. Miragaia, M. Factors contributing to the evolution of mecA-Mediated β-lactam resistance in staphylococci: Update and new insights from whole genome sequencing (WGS). *Front. Microbiol.* **2018**, *9*, 2723. [CrossRef] [PubMed]
27. Wright, G.D. Antibiotic Adjuvants: Rescuing Antibiotics from Resistance. *Trends Microbiol.* **2016**, *24*, 862–871. [CrossRef] [PubMed]
28. Tyers, M.; Wright, G.D. Drug combinations: A strategy to extend the life of antibiotics in the 21st century. *Nat. Rev. Microbiol.* **2019**, *17*, 141–155. [CrossRef] [PubMed]
29. Gibbons, S. Anti-staphylococcal plant natural products. *Nat. Prod. Rep.* **2004**, *21*, 263–277. [CrossRef] [PubMed]
30. Suresh, M.K.; Biswas, R.; Biswas, L. An update on recent developments in the prevention and treatment of Staphylococcus aureus biofilms. *Int. J. Med. Microbiol.* **2019**, *309*, 1–12. [CrossRef] [PubMed]
31. Yang, C.; Saiding, Q.; Chen, W.; An, S.; Zhao, S.; Khan, M.M.; Kong, N.; Ge, M.; Shi, J.; Lin, H.; et al. Chemically modified and inactivated bacteria enable intra-biofilm drug delivery and long-term immunity against implant infections. *Nat. Biomed. Eng.* **2026**, 1–20. [CrossRef] [PubMed]
32. Kannan, S.; Sathasivam, G.; Marudhamuthu, M. Decrease of growth, biofilm and secreted virulence in opportunistic nosocomial Pseudomonas aeruginosa ATCC 25619 by glycyrrhetinic acid. *Microb. Pathog.* **2019**, *126*, 332–342. [CrossRef] [PubMed]
33. Weaver, A.J.; Borgogna, T.R.; Shea-Stone, G.O.; Peters, T.R.; Copié, V.; Voyich, J.; Teintze, M. 18B-Glycyrrhetinic acid induces metabolic changes and reduces staphylococcus aureus bacterial Cell-to-Cell interactions. *Antibiotics* **2022**, *11*, 781. [CrossRef] [PubMed]
34. Wang, Y.; Bian, Z.; Wang, Y. Biofilm formation and inhibition mediated by bacterial quorum sensing. *Appl. Microbiol. Biotechnol.* **2022**, *106*, 6365–6381. [CrossRef] [PubMed]
35. Bronesky, D.; Wu, Z.; Marzi, S.; Walter, P.; Geissmann, T.; Moreau, K.; Vandenesch, F.; Caldelari, I.; Romby, P. Staphylococcus aureus RNAIII and its regulon link quorum sensing, stress responses, metabolic adaptation, and regulation of virulence gene expression. *Annu. Rev. Microbiol.* **2016**, *70*, 299–316. [CrossRef] [PubMed]
36. Vuong, C.; Saenz, H.L.; Götz, F.; Otto, M. Impact of the agr Quorum-Sensing System on Adherence to Polystyrene in Staphylococcus aureus. *J. Infect. Dis.* **2000**, *182*, 1688–1693. [CrossRef] [PubMed]
37. Etter, D.; Jenni, C.; Edwards, V.; Greutmann, M.; Waltenspül, T.; Tasara, T.; Johler, S. Glucose stress lowers staphylococcal enterotoxin C production independently of Agr, SarA, and SigB. *J. Food Prot.* **2023**, *86*, 100127. [CrossRef] [PubMed]

38. Pané-Farré, J.; Jonas, B.; Hardwick, S.W.; Gronau, K.; Lewis, R.J.; Hecker, M.; Engelmann, S. Role of RsbU in controlling SigB activity in Staphylococcus aureus following alkaline stress. *J. Bacteriol.* **2009**, *191*, 2561–2573. [CrossRef] [PubMed]
39. Tran, H.T.; Bonilla, C.Y. SigB-regulated antioxidant functions in gram-positive bacteria. *World J. Microbiol. Biotechnol.* **2021**, *37*, 38. [CrossRef] [PubMed]
40. Kostakioti, M.; Hadjifrangiskou, M.; Hultgren, S.J. Bacterial biofilms: Development, dispersal, and therapeutic strategies in the dawn of the postantibiotic era. *Cold Spring Harb. Perspect. Med.* **2013**, *3*, a10306. [CrossRef] [PubMed]
41. Moormeier, D.E.; Bayles, K.W. *Staphylococcus aureus* biofilm: A complex developmental organism. *Mol. Microbiol.* **2017**, *104*, 365–376. [CrossRef] [PubMed]
42. Zhou, J.; Refat, M.; Guo, Y.; Zhang, J.; Jiao, M.; He, W.; He, X.; Ralbie, M.A.; Ouyang, Z.; Zheng, F. The functional study of response regulator ArlR mutants in staphylococcus aureus. *Appl. Biochem. Biotechnol.* **2024**, *196*, 7687–7702. [CrossRef] [PubMed]
43. Cue, D.; Lei, M.G.; Lee, C.Y. Genetic regulation of the intercellular adhesion locus in staphylococci. *Front. Cell. Infect. Microbiol.* **2012**, *2*, 38. [CrossRef] [PubMed]
44. Kohanski, M.A.; Dwyer, D.J.; Hayete, B.; Lawrence, C.A.; Collins, J.J. A common mechanism of cellular death induced by bactericidal antibiotics. *Cell* **2007**, *130*, 797–810. [CrossRef] [PubMed]
45. Chen, M.; Cui, R.; Hong, S.; Zhu, W.; Yang, Q.; Li, J.; Nie, Z.; Zhang, X.; Ye, Y.; Xue, Y.; et al. Broad-spectrum tolerance to disinfectant-mediated bacterial killing due to mutation of the PheS aminoacyl tRNA synthetase. *Proc. Natl. Acad. Sci. USA* **2025**, *122*, e2412871122. [CrossRef] [PubMed]
46. Hecker, M.; Pané-Farré, J.; Uwe, V. SigB-dependent general stress response in Bacillus subtilis and related gram-positive bacteria. *Annu. Rev. Microbiol.* **2007**, *61*, 215–236. [CrossRef] [PubMed]
47. Zhu, Y.; Weiss, E.C.; Otto, M.; Fey, P.D.; Smeltzer, M.S.; Somerville, G.A. Staphylococcus aureus biofilm metabolism and the influence of arginine on polysaccharide intercellular adhesin synthesis, biofilm formation, and pathogenesis. *Infect. Immun.* **2007**, *75*, 4219–4226. [CrossRef] [PubMed]
48. Simonetti, O.; Rizzetto, G.; Radi, G.; Molinelli, E.; Cirioni, O.; Giacometti, A.; Offidani, A. New perspectives on old and new therapies of staphylococcal skin infections: The role of biofilm targeting in wound healing. *Antibiotics* **2021**, *10*, 1377. [CrossRef] [PubMed]
49. Miller, L.S.; Cho, J.S. Immunity against Staphylococcus aureus cutaneous infections. *Nat. Rev. Immunol.* **2011**, *11*, 505–518. [CrossRef] [PubMed]

Disclaimer/Publisher's Note: The statements, opinions and data contained in all publications are solely those of the individual author(s) and contributor(s) and not of MDPI and/or the editor(s). MDPI and/or the editor(s) disclaim responsibility for any injury to people or property resulting from any ideas, methods, instructions or products referred to in the content.